LA-7009-MS
Informal Report

UC-34b and UC-37

Issued: December 1977

Jupiter Energetic Particle Experiment
ESAD Proton Sensor Design

C. R. Gruhn
P. R. Higbie

los alamos
scientific laboratory
of the University of California
LOS ALAMOS, NEW MEXICO 87545

UNITED STATES
DEPARTMENT OF ENERGY
CONTRACT W-7405-ENG. 36

JUPITER ENERGETIC PARTICLE EXPERIMENT
ESAD PROTON SENSOR DESIGN

by

C. R. Gruhn and P. R. Higbie

ABSTRACT

We describe here a proton sensor design for the Jupiter Energetic Particle Experiment. The sensor design uses avalanche multiplication in order to lower the effective energy threshold. A complete signal-to-noise analysis is given for this design.

In July 1976, NASA released an Announcement of Opportunity (No. 055-3) describing a mission to study Jupiter and its environment by means of a spacecraft orbiting the planet. A particularly important class of particles in the Jovian magnetosphere, which can be studied during this mission, consists of protons having energies from tens of keV to a few MeV. The sensors required for observing such protons must be very rugged to be acceptable for space flight, have as low a threshold as possible, and be able to withstand the large radiation doses produced by energetic electrons and protons in the Jovian magnetosphere. A proposal (LASL # P-717) to measure fluxes of electrons and protons in the environment of Jupiter was prepared and offered ESAD sensors as a possible detector to observe low-energy protons in this environment.

Recent publications[1-4] describe a proton sensor design that offers a number of advantages over the more conventional surface barrier sensor designs. The design proposed as an alternative to a surface barrier sensor is an Epitaxial Silicon Avalanche Diode (ESAD). The ESAD is expected to offer the following advantages:

1. A better signal-to-noise ratio can be achieved for the lowest energy protons to be detected in the presence of a high induced photocurrent, thus a lower proton energy threshold is possible.
2. Because the sensor uses internal amplification (~10), savings are realized in the electronics as follows: a simpler design, less weight, less power, and faster signal processing.
3. The radiation lifetime of the ESAD is expected to be longer (~10^2) than the more conventional surface barrier designs.

The ESAD proton sensor is a 40-μm-thick device, 100 mm^2 in area as shown in Fig. 1. The design consists of an avalanche diode surrounded by a guard diode. The avalanche diode is achieved with a phosphorus diffusion (~1 μm thick) to give an n^{++} region on a 3-Ω·cm, p-type epitaxial layer (~5 μm thick), which is on a second 100-Ω·cm, p-type, epitaxial layer. The net dead layer as viewed by the incident protons is expected to be less than 1500 Å. This layer will just stop 25-keV protons.[5] An optically blocking contact must be achieved on this side of the sensor so that when the sensor views Jupiter the noise associated with the photocurrent is minimal. The major reason for optical transmission of this type of contact is believed to be due to pin holes. This can be avoided by making the evaporation of the contact in a dust-free environment.

The noise associated with this type of photocurrent can be accounted for as follows:

Nyquist noise. The noise-equivalent charge, NEC, is given by:

$$NEC_{Nyquist} = \{\frac{4kTR_s C_p^2}{T}\}^{1/2}, \quad (1)$$

where R_s is the net series resistance to the preamplifier,

C_p is the net parallel capacitance to the preamplifier, and

T is the filter time constant of the shaping amplifier.

Shot noise.

$$NEC_{Shot} = (2qT\{I_0 + I_1 M^2 F(M)\})^{1/2}, \quad (2)$$

where I_0 is the net current not participating in gain,

I_1 is the net current participating in gain and is the sum of a generator current and an induced photocurrent. A typical generator current is $10^{-11} A/mW^2$.

M is the gain,

and $F(M) = 0.028M + (2 - \frac{1}{M})(1 - 0.028)$, which accounts for the difference in ionization coefficients between holes and electrons.

In Table I we show the calculated values of the induced photocurrents for this proton sensor design for light from both Jupiter and starlight. We expect to be able to achieve optically blocking contacts having blocking efficiencies greater than 99.9 percent.

Statistics noise. The noise-equivalent charge associated with the statistical fluctuations in the creation of electron-hole pairs in silicon is given by:

$$NEC_{Fano} = (F \cdot \frac{E}{\varepsilon})^{1/2} \cdot M, \quad (3)$$

where F is the Fano factor and has a value of 0.05[1],

E is the energy deposited in the silicon and ε is the cost to produce an electron-hole pair, $3.62 \pm .02 \frac{eV}{e-h}$ (Ref. 6).

Temperature fluctuation noise. For random changes in temperature we can expect a noise due to gain fluctuations. The noise-equivalent charge associated with this noise source is given by:

$$NEC_{Temp} = 0.002 * \Delta T \cdot \frac{E}{\varepsilon} \cdot M^2, \quad (4)$$

where ΔT is the temperature fluctuation in degrees Kelvin. The coefficient, 0.002, is derived from the temperature coefficient of breakdown voltages for silicon at 300 K.

Gain Nonuniformity. This contribution to the resolution is given by the nonuniformity in gain across the sensor. This contribution adds linearly to the net resolution to the sensor. For this ESAD proton sensor design and assuming "state of the art" material is used, we find

$$\frac{\Delta E(FWHM)}{E} = 0.024 \cdot M. \quad (5)$$

$\Delta E(FWHM)$ is plotted as a function of energy in Fig. 2. This contribution to the resolution is expected to be reduced as the quality of epitaxial material improves. This quality is determined in the control of the uniformity of the resistivity in the epitaxial layers. Selection of material by nondistinctive testing techniques being developed can also insure higher quality.

TABLE I

INDUCED PHOTOCURRENTS IN PROTON SENSOR

Distance From Jupiter	Photon Flux ($cm^{-2}s^{-1}$)	100% Conversion Photocurrent (A)	0.1% Conversion Photocurrent (A)
16 R_J	3.9×10^{13}	2.4×10^{-6}	2.4×10^{-9}
6.5 RJ	2.3×10^{14}	1.4×10^{-5}	1.4×10^{-8}
Starlight	1.2×10^{10}	0.75×10^{-9}	0.75×10^{-12}

The noise-equivalent charge for this noise source is given by

$$NEC_{Gain} = 0.024 \cdot D \cdot \frac{E}{\epsilon} \cdot M^2, \quad (6)$$

where D is the dimension of the avalanche region in cm.

ESAD proton sensor resolution. The total resolution for the proton sensor design is given in Eq. (7).

$$\Delta E(eV,FWHM) = \frac{\epsilon}{M} \cdot \{2.36(NEC^2_{Nyquist} + NEC^2_{Shot} + NEC^2_{Fano} + NEC^2_{Temp})^{1/2} + NEC_{Gain}\}, \quad (7)$$

where all the terms have been defined above. For our calculations we assume the following:

R_s = 50 Ω,
C_p = 256 F,
I_o = 0.0 A (generally small compared to the photocurrent and does not participate in gain),
I generator = 0.0 A (this current is small compared to the photocurrent),
E = 20 keV,
D = 1.0 cm,
T = 300 K, and
ΔT = 1 K.

In Fig. 3 we show the results of this calculation where we assume only Nyquist and shot contributions to the noise as a function of the filter time constant. Figures 4 and 5 show the resulting resolution (all contributions included) as a function of the filter time constant and gains of 10 and 20, respectively. For induced photocurrents (10^{-7}A), the optimum filter time constant appears to be 300 ns. A signal-to-noise ratio of 3/1 at a gain of 10 and at this filter time constant is expected for this design.

Figure 6 shows the equivalent calculation for a surface barrier detector geometry. Table II summarizes the main differences between the surface barrier detector design and the ESAD proton sensor design. For kilovolt protons and photocurrents $<10^{-7}$A, equivalent signal-to-noise ratios are achieved for the two designs. The main differences are:

1. The ESAD design requires an optimum lifter time constant of 3×10^{-7}s, as compared with 4×10^{-6}s for the surface barrier design.
2. The signal and noise is ten times larger for the ESAD as opposed to that achieved in surface barrier design.

For a 20-keV proton, and using a gain of 20, the signal is $\sim 10^{-14}$C at the input of the preamplifier. This large amount of charge at the input of the electronic chain is expected to yield a simplification in design which results in less electronics, less weight, and less power.

Temperature stability during operation of the ESAD sensor does not appear to be critical. This contribution to the resolution is given by

$$\frac{\Delta E}{E} = -2 \times 10^{-3} M/^oC. \quad (8)$$

TABLE II

COMPARISON OF DESIGN FEATURES

	Surface Barrier Design	ESAD Design
$\Delta E(I_{photo} = 10^{-6}A)$	16 keV	11 keV
Tmin	1.5×10^{-6}s	1.0×10^{-7}s
$\Delta E(I_{photo} = 10^{-7}A)$	8.8 keV	8.0 keV
Tmin	4×10^{-6}s	3.0×10^{-7}s
Signal (20 keV)	5.6×10^{3}e	5.6×10^{4}e
$NEC(I_{photo} = 10^{-7}A)$	2.4×10^{3}e	2.2×10^{4}e

From a survival viewpoint the ESAD proton sensor is sturdier than the conventional surface barrier sensor. During ground testing and spacecraft integration, sensors are often subjected to unavoidable temperature extremes and are exposed to atmospheric contaminates. Temperature cycling, which can affect the characterization of a surface, is less of a problem for the ESAD. The radiation lifetime of the ESAD is expected to be longer because of the lower resistivity material used in the design.

As the "state of the art" in growth of epitaxial silicon improves, we can expect improvements in the achievable signal-to-noise ratio in the ESAD sensor design. Ultimately, the results in Fig. 3 should be realized, yielding a limiting signal-to-noise ratio of 6/1 for a photocurrent of 10^{-7}A (compared to 2.2/1 for surface barrier design).

REFERENCES

1. C. R. Gruhn, "Epitaxial Silicon Semiconductor Detectors, Past Developments, Future Prospects," IEEE Trans. Nucl. Sci. NS-24, (February 1977).
2. C. R. Gruhn, "A Thin All Epitaxial Silicon Detector with Internal Amplification," IEEE Trans. Nucl. Sci. NS-23, 145-152, (February 1976).
3. C. R. Gruhn, S. Depp, Nelson Jarmie, and P. W. Keaton, "Nonlinear Aspects of the Avalanche Gain Mechanism in Silicon Avalanche Diodes," Nucl. Insts. and Meth. (to be published).
4. P. P. Webb and R. J. McIntyre, "Large Area Reach-through Avalanche Diodes for X-ray Spectroscopy," IEEE Trans. Nucl. Sci. NS-23, 138-144, (February 1976).
5. ARL 64-151 (June 1964).
6. F. E. Emery and T. A. Ralson, "Average Energy Expended Per Ionized Electron-Hole Pair in Silicon and Germanium as a Function of Temperature," Physical Review 140, 2089-2-93 (December 1965).

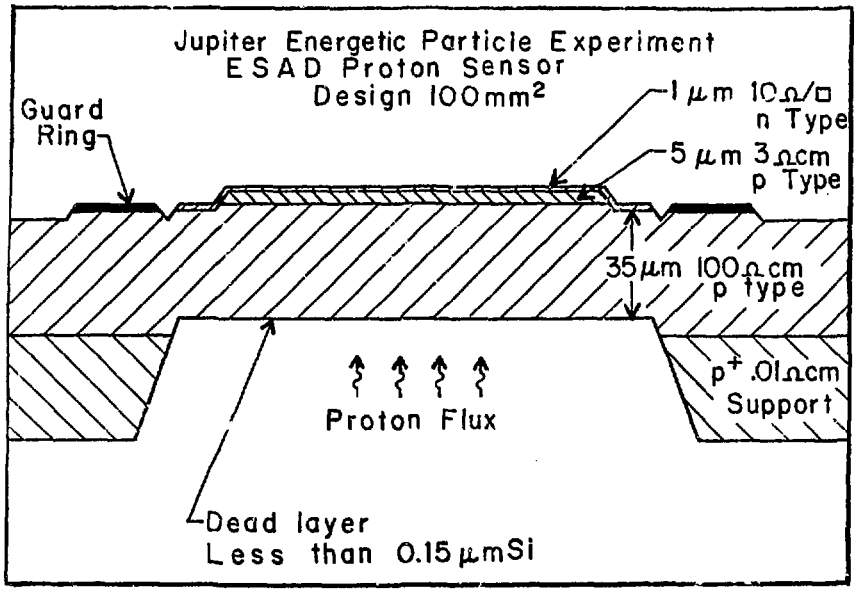

Fig. 1. ESAD proton sensor design.

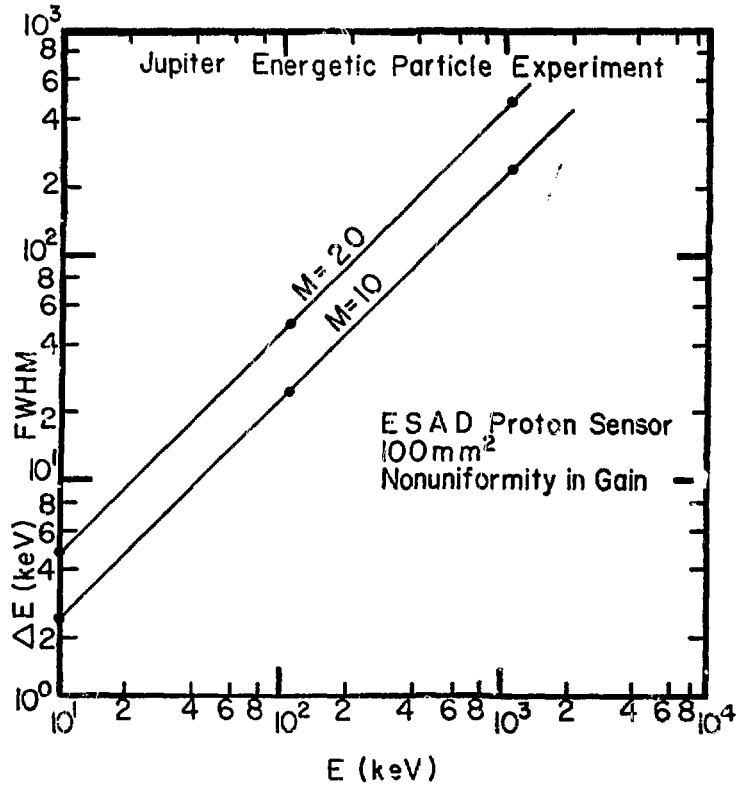

Fig. 2. Gain nonuniformity contribution to the resolution ΔE(keV FWHM) vs. energy E(keV) and gain M.

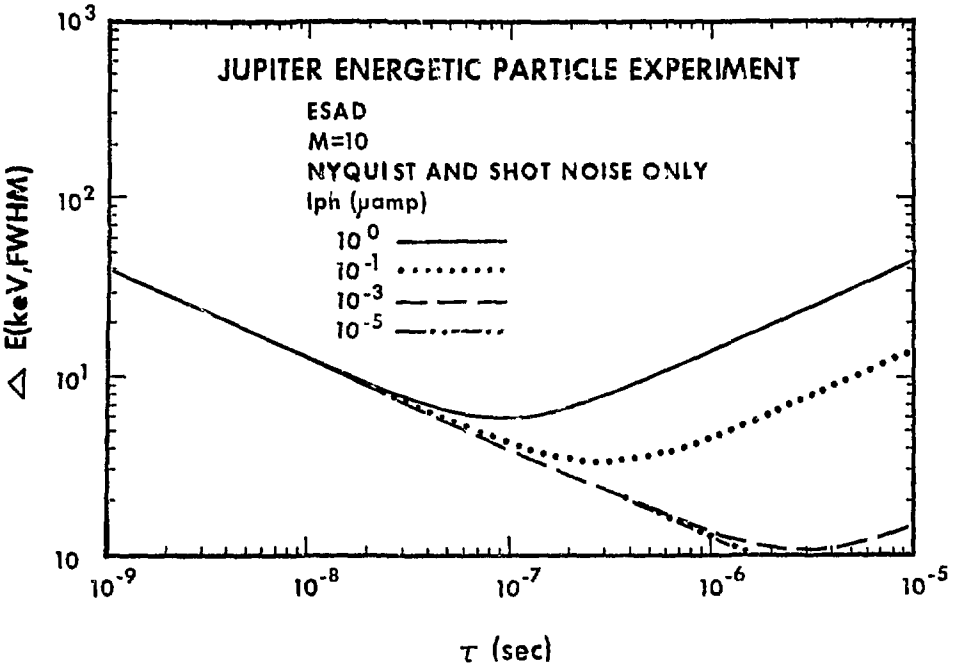

Fig. 3. Nyquist and shot contributions to the noise as a function of the filter time constant.

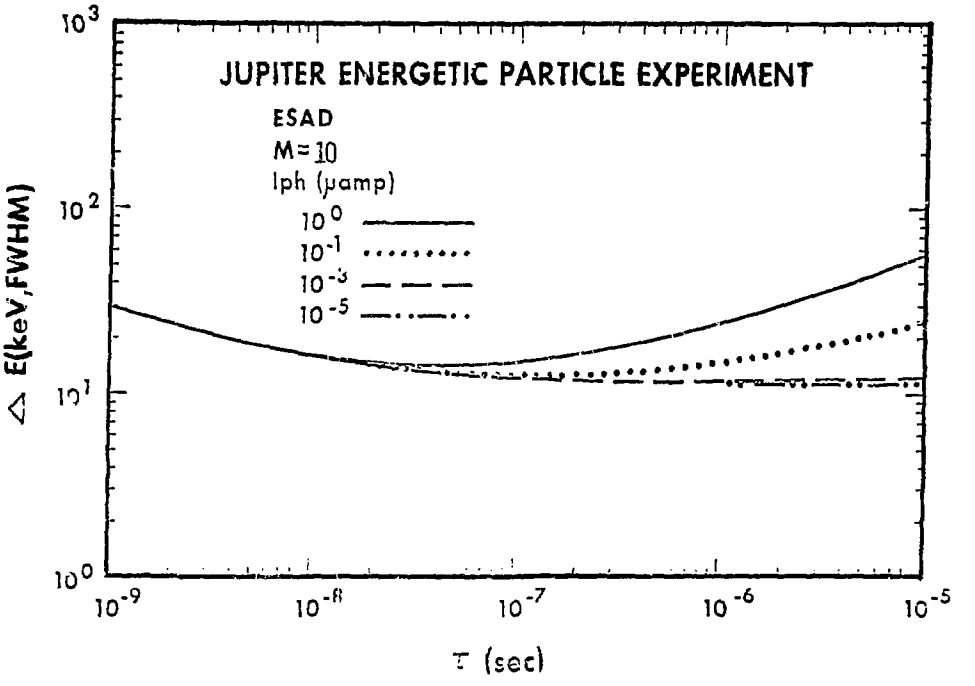

Fig. 4. Resolution (all contributions) as a function of the filter time constant for a gain, M = 10, and various photocurrents.

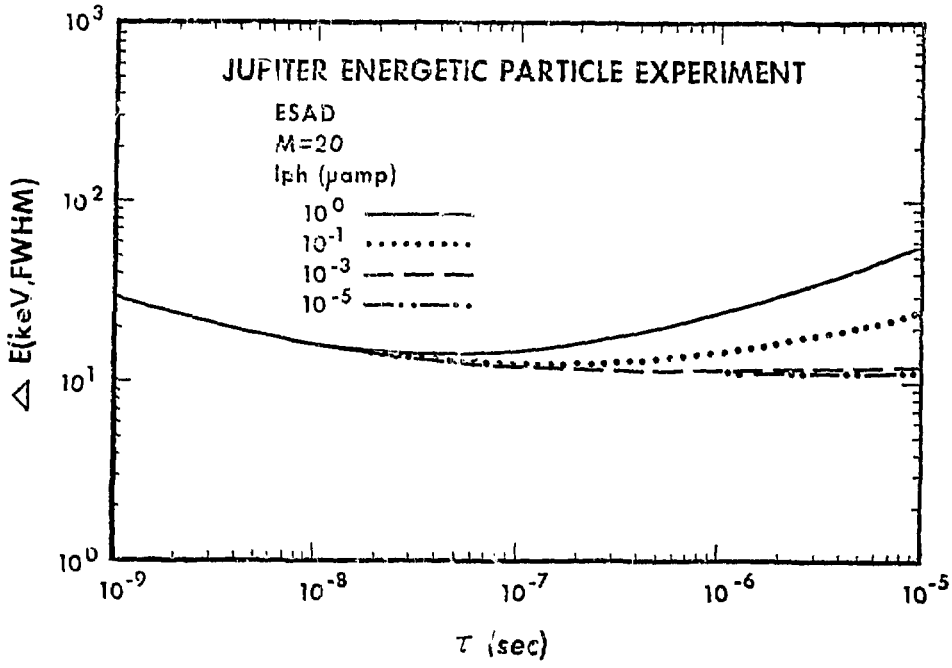

Fig. 5. Resolution (all contributions) as a function of the filter time constant for a gain, M = 20, and various photocurrents.

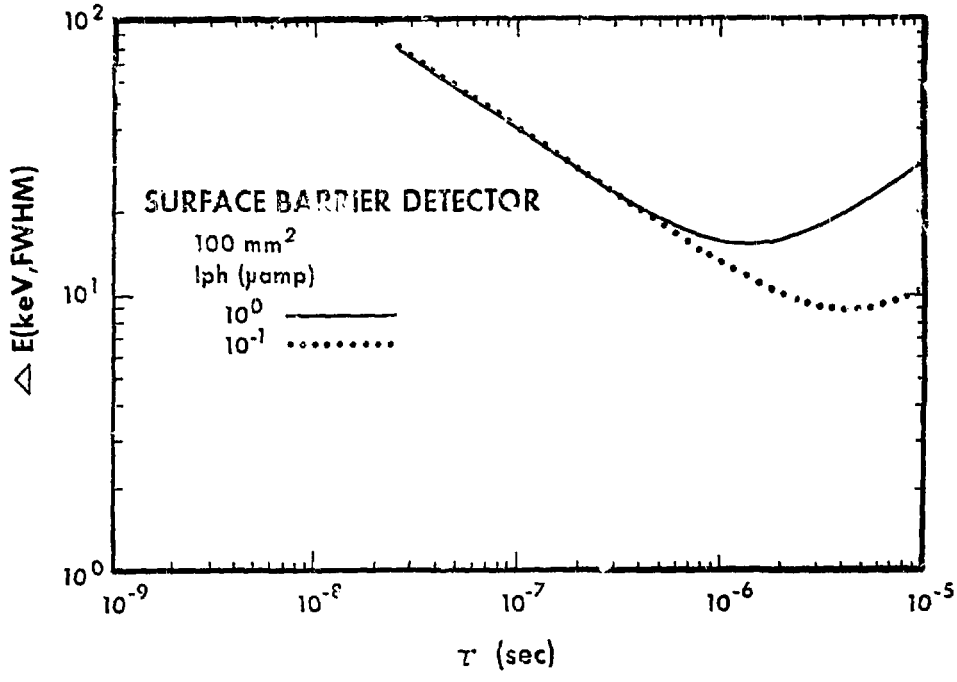

Fig. 6. Resolution (all contributions) of conventional surface barrier detector as a function of the filter time constant and photocurrent.